

Formation and evolution of Pluto’s small satellites

Kevin J. Walsh, Harold F. Levison

Southwest Research Institute, 1050 Walnut St. Suite 300, Boulder, CO 80302, USA

`kwalsh@boulder.swri.edu`

ABSTRACT

Pluto’s system of 5 known satellites are in a puzzling orbital configuration. Each of the four small satellites are on low-eccentricity and low-inclination orbits situated near a mean motion resonance with the largest satellite Charon. The Pluto-Charon binary likely formed as a result of a giant impact and so the simplest explanation for the small satellites is that they accreted from debris of that collision. The Pluto-Charon binary has evolved outward since its formation due to tidal forces, which drove them into their current doubly synchronous state. Meanwhile, leftover debris from the formation of Charon was not initially distant enough from Pluto-Charon to explain the orbits of the current small satellites. The outstanding problems of the system are the movement of debris outward and the small satellites location near mean motion resonances with Charon.

This work explores the dynamical behavior of collisionally interacting debris orbiting the Pluto-Charon system. While this work specifically tests initial disk and ring configurations designed to mimic the aftermath of the disruption of satellites by heliocentric impactors, we generally find that collisional interactions can help move material outwards and keep otherwise unstable material dynamically bound to the Pluto-Charon system. These processes can produce rings of debris whose orbits evolve rapidly due to collisional processes, with increasing pericenters and decreasing semimajor axes. While these rings and disks of debris eventually build satellites significantly further out than the initial locations of a disrupted satellite, they do not show a strong preference for building satellites in or near mean motion resonances with Charon under a wide array of tested conditions.

Subject headings: minor planets, asteroids: formation — Kuiper Belt objects: general — planets and satellites: dynamical evolution and stability

1. Introduction

Charon is the most massive satellite in the Solar System relative to its primary’s mass, with $M_{\text{Charon}} = 0.1126M_{\text{Pluto}}$ (Beauvalet et al. 2013). It is a doubly synchronous system, with rotational and orbital periods of 6.38 days, orbiting on a near-zero eccentricity orbit with semimajor axis $a_{\text{Charon}} = 19596$ km, which is $\sim 17 R_{\text{Pluto}}$ (Stern et al. 2003, Buie et al. 2012, Brozović et al. 2014). Pluto has at least four smaller satellites, each orbiting with a period that is near an integer ratio of Charon’s period and at distances between 30–60 R_{Pluto} (Weaver et al. 2006, Buie et al. 2006, Stern et al. 2007, Showalter et al. 2011, Showal-

ter et al. 2012, Buie et al. 2013, Brozović et al. 2014). Their orbits are estimated to be nearly circular ($e < 0.01$), and co-planar ($i < 1^\circ$) (Brozović et al. 2014).

While there are doubly synchronous binary asteroid systems with even higher mass ratios (where satellite mass divided by primary mass is closer to 1; Main Belt Asteroid (90) Antiope and Trojan Asteroid (617) Patroclus are both nearly similarly sized; Richardson and Walsh 2006), the seemingly delicate dynamics of the system of small satellites are not found duplicated among asteroid satellite systems. Meanwhile the extreme size of Charon relative to Pluto makes it unique in the Solar Sys-

tem relative to planetary satellites, but the system has some similarity, at least in complexity, to Saturn’s system. Some works, including this one, envision the small satellites forming from a disk or ring of debris. This disk would differ from Saturn’s rings, or the recently discovered rings around the Centaur (10199) Chariklo (Braga-Ribas et al. 2014), as it would be entirely outside the Roche Limit of Pluto where Styx, the innermost small satellite, is over 10 times further from Pluto than its nominal Roche Limit. Therefore particles could accrete into large satellites once relative velocities became low on timescales that are fast compared to viscous stirring timescales.

1.1. Physical and Orbital Properties

Brozović et al. (2014) reported the best fits for the orbital properties of Nix, Kerberos and Hydra, based on multiple Hubble Space Telescope observing campaigns (Table 1; see also Buie et al. 2013). Of particular importance to this study are the period ratios between each satellite and Charon; 3.1565, 3.8913, 5.0363, 5.9810 for Kerberos, Nix, Kerberos and Hydra (Brozović et al. 2014). From these data it appears that none of the satellites are currently in resonance with Charon or each other, and they are not systematically on the inside or outside of resonance, nor do their distances from resonance correlate with size.

The physical properties of the small satellites are difficult to estimate since imaging is limited to optical wavelengths and photometric measurements can determine size only with an estimate for each bodies’ albedo, and mass only with an estimate for density and size. Orbital stability has been used to place limits on masses of both hypothetical satellites (pre-discovery) and also for subsets of the current system. Stern et al. (1994) studied the stability of hypothetical satellites in the Pluto-Charon system, primarily placing an upper limit on satellite mass, $3 \times 10^{-4}(M_{\text{Pluto}} + M_{\text{Charon}})$, that would create observable perturbations in Charon’s orbit. Following the discovery of Nix and Hydra, Pires dos Santos (2011) tested for stable regions where more satellites could reside assuming masses of 5.8×10^{17} kg and 3.2×10^{17} kg for Nix and Hydra respectively (using masses from Tholen et al. 2008). With these masses the stable region between those satellites is quite narrow and centered around the 5:1 MMR – the location

where Kerberos was eventually found.

Youdin et al. (2012) presented a series of numerical experiments attempting to constrain the mass of the larger satellites (Nix and Hydra) by considering the long-term survival of Kerberos, orbiting between them. This work suggested that period ratios for Kerberos relative to Charon were more stable below 4.98 and above 5.01, which agrees with the recent period ratios estimate (5.0363) from Brozović et al. (2014). Upper limits for mass found in that work, $M_{\text{Nix}} \lesssim 5 \times 10^{16}$ kg and $M_{\text{Hyd}} \lesssim 9 \times 10^{16}$ kg, which required that the satellites have an albedo above 0.30 for the assumption of an internal density of 1 g cm^{-3} .

The orbital fits by Brozović et al. 2014 also constrained the masses of individual satellites. The larger satellites were found to have masses $M_{\text{Nix}} = 4.5 \times 10^{16}$ kg and $M_{\text{Hyd}} = 4.7 \times 10^{16}$ kg, which are both similar and within a factor of two respectively from that found in Youdin et al. (2012). The estimated mass for Kerberos is $M_{\text{Kerberos}} = 1.6 \times 10^{16}$ kg. Using a range of possible visible albedo (35%–4%), this work estimated radii ranges for all four satellites: 4–14 km, 23–70 km, 7–22 km, and 29–86 km for Styx, Nix, Kerberos and Hydra respectively.

Satellite	a (km)	a (R_{Pluto})	e	i (deg)	P (days)	P_{sa}
Charon	19596	16.59	0.00005	0.0	6.3872	1
Styx	42413	35.91	0.00001	0.0	20.1617	3.1
Nix	48690	41.22	0.00000	0.0	25.8548	3.8
Kerberos	57750	48.89	0.00000	0.4	32.1679	5.0
Hydra	64721	54.80	0.00554	0.3	38.2021	5.9

Table 1: Orbital elements for all satellites and for the radii of the small satellites are from Brozović et al. (2014). Charon’s diameter is from occultation measurements (Sicardy et al. 2006). Pluto’s radius, 1181 km, for a/R_{Pluto} estimates from Lellouch et al. (2009). Charon’s orbital elements are plutocentric, while the small satellites orbital elements are relative to the Pluto-Charon barycenter.

1.2. Formation of Charon and debris

Charon is thought to have formed in a giant impact (McKinnon 1989, Canup 2005,2011). SPH simulations show that it likely remained intact following the collision, making it a prototype for an “intact capture” type of high impact-parameter

collision event (Canup 2005). Formation from a disk following the impact appears to still be dynamically possible (Canup 2005), but the intact capture is preferred due to the fact that Charon has a similar density as Pluto. More violent events that result in the accretion of Charon from a circum-Pluto disk (similar to the Earth-Moon scenarios) lead to the loss of rocky material to Pluto and create larger density disparity between Pluto and Charon (see Desch 2014 for a model to preserve density similarities during the formation of Charon from a disk).

The high angular momentum of the system, and its doubly synchronous state, point to past tidal evolution from a closer orbit of Charon around a more rapidly rotating Pluto (Farinella et al. 1979, McKinnon 1989, Dobrovolskis et al. 1989, Cheng 2011). The SPH models of the Charon-forming event that satisfy these angular momentum constraints typically find that its orbit would initially have been eccentric (Canup 2005, 2011). The possible post-collision orbits for Charon are discussed in detail in Canup (2005,2011), where the initial orbits range between semimajor axes of 4–10 R_{Pluto} , with eccentricities between 0.1–0.8 (see Fig 5. Canup 2011). There are also simulations that produce $e \sim 0.9$ with $a/R_{\text{Pluto}} \sim 25$.

Peale et al. (2011), Cheng (2011) and Cheng et al. (2014a), show that the tidal evolution of Charon required a few million years to reach its current semimajor axis with variations in the orbit evolution dominated by the choice of tidal models. These recent works consider an initially eccentric orbit for Charon as predicted in the “intact capture” formation models and they find similar evolution timescales as previous estimates for Charon evolving on a circular orbit (Farinella et al. 1979, Dobrovolskis et al 1989, Peale 1999). Solutions where the eccentricity of Charon remained moderate were desirable outcomes to test the viability of resonant transport of the satellites in the co-rotation resonance with Charon (Ward and Canup 2006, Lithwick and Wu 2008, Cheng 2011, Cheng et al. 2014a,b). Cheng et al. 2014a find for Charon to remain moderately eccentric during its tidal evolution the ratio of dissipation between Pluto and Charon has different values depending on the tidal model used. However, for a range of these parameters, both tidal models tested by Cheng et al. 2014a find evolutions where Charon

has $e \sim 0.1$ – 0.5 for the entire outward evolution, only damping to 0 when Charon has reached its current semimajor axis.

There are alternative orbital evolutions due to different initial conditions or tidal parameters. For example, Canup (2011) finds some collision simulation outcomes where Charon has a semimajor axis close to where it is found today, but with a much larger eccentricity (see Figure 5 of Canup 2011). Similarly, if the tidal dissipation parameters were substantially different than those used in the calculations the timescale for the evolution could change. While these extremes are not essential for the work presented here and therefore not discussed in depth, it is possible that other mechanisms for explaining the small satellites may require them.

Canup (2011) characterized the debris created in the “intact capture” models in terms of the mass and maximum equivalent circular orbit of disk material ($a_{\text{eq,max}}$), where a_{eq} is the circular orbit containing the same amount of angular momentum, and $a_{\text{eq,max}}$ is the maximum value for all debris in the simulation (see Fig 6.). The total mass of debris was typically between 10^{17} – 10^{21} kg on orbits between $a_{\text{eq}}=2$ – $30 R_{\text{Pluto}}$, with no clear correlation between the two. Typical orbits of post-impact Charon are eccentric with $a \sim 4$ – $10 R_{\text{Pluto}}$. Holman and Weigert (1999) studied stability around binary systems and find that in a best-case scenario of zero eccentricity for both Charon and the debris the closest stable orbit is at $\sim 1.974 a_{\text{Charon}}$. For a nominal formation outcome of $a_{\text{Charon}} \sim 4$ – $10 R_{\text{Pluto}}$, debris closer than $a_{\text{Charon}} \sim 8$ – $20 R_{\text{Pluto}}$, would be immediately unstable. If Charon had an initially eccentric orbit then the nearest stable orbit is further away with less debris being stable.

The current orbits of the small satellites (~ 30 – $60 R_{\text{Pluto}}$), are much further from Pluto than any of the debris in the simulations of Canup et al. (2011), and thus it is unlikely that today’s satellites formed directly on today’s orbits during the formation of Charon. Any satellites formed during the formation of Charon would later witness its outward tidal evolution. As Charon moved outward the locations of its mean motion resonances would also move and would sweep over the orbits of any existing satellites. Mean motion resonances with Charon would perturb or capture satellites

resulting in rapid and destabilizing eccentricity excitement (Ward and Canup 2006). Since tidal forces are far too weak to damp the current satellites eccentricities (Stern et al. 2006), their near zero eccentricity orbits also suggest that they did not witness the tidal evolution of Charon in their present configuration.

A corotation resonance capture has been proposed as a means to transport satellites without exciting their eccentricities (Ward and Canup 2006). This resonance capture requires a moderate eccentricity for Charon during its outward migration. However, the restrictions on the corotation resonance is that transport in resonance requires a narrow range of eccentricity for Charon for each different resonance, and for multiple satellites these requirements are probably mutually exclusive (Lithwick and Wu 2008, Cheng 2011, Cheng et al. 2014b). With a moderate or large eccentricity for Charon it is also possible to capture a satellite in multiple resonances at once and keep a relatively low eccentricity for the satellite. However, this was found to be an extremely low probability event and also ineffective for the inner resonances where Styx and Nix are found (Cheng 2011, Cheng et al. 2014b).

Kenyon and Bromeley (2014) estimate that primordial debris from the Pluto-Charon forming collision would, by way of a collisional cascade, reach stable orbits just outside the region of orbital instability caused by Charon’s orbit. This ring would then spread on timescales of 5–10 years due to the tidal input of angular momentum into an optically thick disk. These short timescales, if less than accretion timescales, could permit spreading of the ring into a disk before accretion begins. An essential aspect of the analytical estimate of the spreading time is that angular momentum transfer among ring particles slows their precession, which helps to maintain low-velocity collisions. This avoids collisional fragmentation on timescales short compared to that for spreading. However, Kenyon and Bromeley (2014) do not account for the fact that low-velocity collisions will simply result in accretion and growth. Rather, accretion will likely happen before spreading and a disk will not form, something that is found in simulations presented below in Section 4. The timescales for this disk spreading and satellite growth proposed by Kenyon and Bromeley (2014) are faster than

the tidal evolution of Charon. Any satellite system formed in this manner, immediately following the formation of Charon, would then be subjected to the sweeping resonances caused by Charon’s outward tidal evolution that would induce significant eccentricities into the small satellites.

Material can also be captured from heliocentric orbit. Two passing objects colliding within the Hill Sphere of the Pluto-Charon system can result in capture of some of the collisional debris (Pires dos Santos et al. 2012). The total amount of captured material depends on the orbital and size distributions of the passing material. Pires dos Santos et al. (2012) explored this mechanism finding that large objects that would carry significant mass have collision timescales that are too long, resulting in a very small total amount of captured mass.

How the present satellites or their building blocks got to where they are today is still an open question. The capture of material from outside the Pluto-Charon system is inefficient, and moving the present day satellites in various arrangements of orbital resonances has not been demonstrated. Moving a single satellite outward may be possible (Lithwick and Wu 2008; see also Cheng 2011, Cheng et al. 2014b), and some eccentricity excitement would be irrelevant if the transported satellite simply served as the source material for the entire suite of today’s satellites (of course too much eccentricity excitement can lead to dynamical ejection or accretion by Pluto or Charon). A satellite disrupted after the tidal evolution of Charon could form a collisionally active disk as envisioned by Kenyon and Bromeley (2014). But growth of satellites from a collisionally damped disk does not imply growth near mean motion resonances, as Kenyon and Bromeley (2014) found no strong preference for growth in those locations.

The breakup of a satellite may also form an eccentric ring, which could have strong dynamical interactions with Charon at the same time as it is collisionally evolving. Similarly, the disruption of a primordial satellite *during* the tidal evolution of Charon could have interactions with Charon while it is still on an eccentric orbit. If a satellite is disrupted it will be important if the dynamical environment forces it to re-accrete in a new location. If the timescale for the disruption and reaccretion of a satellite is short compared to

the tidal evolution of Charon, then it is a process that could be repeated multiple times. This could be a way to avoid dynamical ejection of a satellite as repeated disruption and re-accretion events could help it avoid interacting with the strongest resonances that sweep outward as Charon’s orbit expands. What happens during its disruption, its evolution as a ring or disk of debris and its reaccretion into a new satellite could then be important. Here we endeavor to study the evolution of debris following the disruption of a satellite.

1.3. The role of collisional evolution

The state of the Kuiper Belt at the time of the Charon-forming collision is important for determining the collisional environment of the Pluto-Charon system during and after its formation. The giant impact that formed Charon was the last giant impact on Pluto, but must characterize a substantially different collisional environment in the Kuiper Belt than is found today. Today the chance of such a collision is essentially zero (Brown et al. 2007). Meanwhile the tidal evolution of Charon was relatively short compared to timescales for dynamical mixing and depletion of the Kuiper Belt (Levison et al. 2008), and thus an enhanced collisional environment may have persisted throughout the entire tidal evolution. In this study we will repeatedly refer to this idea and consider the possibility that small satellites ($D < 100$ km) in the Pluto-Charon system may have had a very short collisional disruption timescales in the epoch immediately following the Charon-forming event and *during* the tidal evolution of Charon.

Collisional interactions between particles in the system will change their dynamical evolution by damping of excess energy and changing particles orbits. A satellite experiencing isotropic collisions in orbit will experience a damping of its radial velocity, decreasing eccentricities. Meanwhile angular momentum of the system is conserved among a collisionally active swarm, so while orbits will evolve to lower eccentricity, e , the value of $a \times \sqrt{1 - e^2}$ is conserved for the population of particles resulting in decreased semimajor axis a , and increased pericenter $q = a(1 - e)$. Orbits with lower e and larger q are more stable and longer-lived in the Pluto-Charon system, and so even small amounts of collisional evolution may

be important for increasing lifetimes of satellites or debris.

In this work we focus on the role that collisional evolution could play in both the transport of material outward during the tidal evolution of Charon, and also during the accretion of satellites following the conclusion of tidal evolution. Unlike previous works we examine the outcome of satellite disruption around a tidally evolving Charon and the formation and evolution of the eccentric ring of debris. For collisional processes to be important there must have been collisions, and material or debris in enough quantity to affect the evolution of the system. Specifically we assume, and then explore the idea, that the current satellites we see today are built from the pieces of previous disrupted satellites.

In Section 2 we explore stable orbits in $a - e$ space around Pluto-Charon systems with different eccentricity for Charon’s orbit since tidal evolution models allow for a range of eccentricities. In Section 3 we explore the collisional evolution of a few simple idealized disks of particles. Finally, in Section 4 we model the evolution of the debris of a disrupted satellite, and compare this evolution among systems with different eccentricities for Charon’s orbit, and also around a system with a single central body.

2. Stability of orbits in the Pluto/Charon system

The long term stability of a particle around the Pluto-Charon pair depends on the particle semimajor axis and the eccentricity of both it’s orbit and that of Charon. The innermost stable orbit, often cited as a critical semimajor axis (a_{crit}), is a value that has been explored in detail in previous numerical and analytical work. Holman and Weigert (1999) produced an empirical fit for the a_{crit} as a function of orbital eccentricity (e) and reduced mass ($\mu = M_2/(M_1 + M_2)$). Using the Pluto-Charon reduced mass $\mu = 0.104$ this simplifies to the following formulation, $a_{\text{crit}} = 1.974 + 4.65e - 2.17e^2$.

Of particular interest for the origin of the small satellites of Pluto are regions of stability while Charon is tidally evolving, during which Charon could have a range of non-zero eccentricities. We have explored stability limits for the Pluto-Charon

mass ratios, seeking not just the innermost stable orbit, but the envelope of allowable eccentricities as a function of distance from Pluto-Charon for a range of Charon eccentricity.

We include tests for Charon eccentricity between 0.0–0.3, in steps of 0.1 and consider initial test particle eccentricities ranging from 0–0.7, and initial semimajor axes that ranged from 1.35–5.1 a_{Charon} with randomized orbital angles (see Fig 1). The tests were simulated for 1000 years using the `swift_symba5` numerical integrator (Duncan et al. 1998) with a timestep of 2×10^{-4} years (1.75 hours, which is $\sim 1/87$ th Charon’s orbital period). We consider co-planar or nearly co-planar cases as the observed system of small satellites all appear to be very close to co-planar (see also Pires dos Santos et al. 2011, who considered some small inclination variations in similar tests).

For each of the tested eccentricity values of Charon, $e = 0.0 - 0.3$, the formulation of Holman and Weigert (1999) yields $a_{\text{crit}} = 1.97, 2.41, 2.81, 3.17 a_{\text{Charon}}$. These values were found to agree with those found by Dvorak et al. (1989). The simulations performed here find similar innermost stable orbits. For Charon on a circular orbit we find virtually no stable orbits inside of the 3:1 MMR ($\sim 2.08 a_{\text{Charon}}$; see Fig 1), near $1.97 a_{\text{Charon}}$ as found in the Holman and Weigert work. Meanwhile, at the location of the furthest known satellite, Hydra, near the 6:1 MMR, particles are unstable with $e > 0.35$.

We have made an empirical fit to the stable region when $e_{\text{Charon}} = 0$ with a curve described by $e < (1 - (1.7a_{\text{Charon}}/a))^{(5/3)}$. We use this curve throughout the later sections as a guide for when regions of an eccentric disk are on unstable orbits.

Cases where Charon has an eccentricity of 0.3, the stability region is truncated near the 5:1 MMR (at $2.9 a_{\text{Charon}}$, similar to the Holman and Weigert 1999 value of $3.17 a_{\text{Charon}}$). Lower eccentricities are generally required for stability, with a particle near the 6:1 MMR requiring $e < 0.25$ for this case. We estimate the boundary of this stable region with the following empirical curve, $e < (1 - (2.2a_{\text{Charon}}/a))^{(5/3)}$ and $a > 2.9 a_{\text{Charon}}$.

[EDITOR: Place Fig 1 here]

An important aspect of this result is that particles with an eccentricity above the established a - e curve are unstable on short timescales. However,

if their collisional timescale is shorter, then a series of collisions need only to decrease their orbital eccentricity below these stability limits to keep them in the system for long times. Another implication of this experiment is that while Charon has a high eccentricity, at times as high as 0.3 as suggested by Peale (2011), the current orbits of Nix, P4 and P5 would not be stable. Thus, we could expect that these bodies formed after the eccentricity damping of Charon or were in a stable resonant state that increased their stability. We did not find such stable resonant states in this work, but did not design experiments specifically for that purpose. Cheng (2011) and Cheng et al. (2014b) explored the behavior of particles in multiple resonances and struggled particularly to find stable cases in the 4:1 resonance.

3. Evolution of Collisionally evolving disks

In this section we model a series of eccentric rings of debris and we track their different dynamical evolution as a function of different collisional environments. The role of Charon in changing the evolution of the disk is explored by alternatively placing some disks around single bodies with the combined mass of Pluto and Charon. We model the collisional interactions of the ring particles and their effects on the ring’s eccentricity and semimajor axis.

Required for these tests are the calculations of inter-particle collision outcomes. The frequency and outcome of collisions are strongly dependent on relative particle sizes, total system mass and orbital distributions, all of which can change rapidly owing to accretion, fragmentation and gravitational interactions with Charon. Statistical calculations must be made in order to model high collisional frequencies possible for populations of small particles. If each particle were included directly in a simulation the total number of particles (N) of any calculation would be overwhelmingly large. However, the dynamics of capture in MMR and interactions with Charon demand that the simulation also accurately model the gravitational dynamics, where timescales are controlled by the orbital period of Charon.

The primary code we employ is LIPAD, which stands for Lagrangian Integrator for Planetary Accretion and Dynamics (Levison et al. 2012). It

is based on the efficient integration techniques known as the Wisdom-Holman Mapping (WHM; Wisdom & Holman 1991), and specifically SyMBA that has the added property of treating close encounters between bodies (Duncan et al. 1998).

In order to represent the extremely large number of particles required LIPAD relies on “tracer” particles. Each of the tracer particles represents a large number of comparably-sized particles on very similar orbits. Each tracer is defined by three quantities, the physical radius s , the bulk density ρ and the total mass of particles that the tracer represents m_{tr} . Throughout the simulation m_{tr} and ρ do not change. When fragmentation and accretion are included the radius s can change and thus the number of particles that the tracer represents will change as a function of s , with $N_{\text{tr}} = m_{\text{tr}}/(4/3)\pi\rho s^3$. For all of the work presented here, the density of each tracer is set at 1 g cm^{-3} .

Collisional probabilities for tracers are calculated for each tracer as a function of its size s and the total mass, sizes and orbits of its neighbors using particle-in-a-box algorithms. The outcome of the collision then affects the tracer particle itself, as though it were a planetesimal of radius s , so that each tracer is tracing the behavior of the system (see Section 2.1.1 of Levison et al. 2012 for more details on the tracer-tracer interactions). Meanwhile the dynamics of each tracer is modeled with gravity calculations and other effects that are handled statistically (dynamical friction, viscous stirring), some of which depend on the particle’s radius s and the masses, sizes and orbits of its neighbors.

A particular advantage for this problem is that the Lagrangian nature of the code enables it to model eccentric rings (see Levison and Morbidelli 2007, Levison et al. 2012). When a tracer is determined to have collided with another particle, it is necessary to determine the properties of the impactor. The orbit that the impactor would have had prior to impact is determined by tracking particles that have most recently inhabited the correct regime of semimajor axis a and radius s . From this list of possible impactors the one with the closest true anomaly is selected, which was shown by Levison and Morbidelli (2007) to be critical to support asymmetries and eccentric rings.

When collisions occur LIPAD uses a fragmen-

tation law based on Benz & Asphaug (1999) to determine the outcomes. This fragmentation law determines the expected size distribution of fragments, but the entire distribution is not assigned to either tracer - rather a radius s is chosen for each from the distribution. The system’s size distribution is built from a number of tracer particles with different sizes s , and matches standard collisional evolution codes owing to the statistical nature of the radius selection from a large number of collisions (see Levison et al. 2012).

For the cases presented in this Section the collisional fragmentation and growth of particles is not used, rather we simply explore the role of collisional damping.

The first test case, dubbed “simple eccentric disk”, is designed to examine how the perturbations of Charon change the evolution of a collisionally active disk at distances similar to the current small satellites. This test begins with a coplanar disk of particles with the same semimajor axis $a = 3.05 a_{\text{Charon}}$ and eccentricity $e = 0.2$, and randomized orbital angles (see Fig 2a). The semimajor axis is just beyond the 5:1 MMR, which is located at $\sim 2.9 a_{\text{Charon}}$. The equivalent circular orbit of disk material (a_{eq}) is inside the 5:1 MMR at $\sim 2.85 a_{\text{Charon}}$, meaning that removal of orbital energy by collisional damping, while conserving angular momentum would result in a ring at this lower semimajor axis orbit. All of the particles are initially within the stability boundaries defined above in Section 1, and are therefore stable for long timescales. The simulations used 10,000 particles, where each has a mass of 1.02×10^{14} kg (totalling $\sim M_{\text{Nix}} + M_{\text{Hydra}}$ from Buie et al. 2008). Three simulations were run, where the tracer particles’ representative radii were varied to be $R=0.3, 0.1$ or 0.01 km (meaning $N_{\text{tr}} = 8 \times 10^8, 2.4 \times 10^9, 2.4 \times 10^{10}$ respectively). Charon’s eccentricity was ~ 0.2 throughout and it was at its current semimajor axis.

For the case of $R = 0.1$ km (illustrated in Fig 2) the ring experiences rapid gravitational evolution due to interactions with Charon. The eccentricity distribution is spread out with values reaching as high as 0.4 in just a few Charon orbits. Collisional damping is also dramatic for these conditions and are on similar timescales. After a few Charon periods many particles are experiencing damping with their eccentricities decreasing to near 0. For

these conditions the damping effects are powerful enough to decrease all particle eccentricities on year timescales. After this time nearly all particles have eccentricities below their initial value of 0.2 and the disk reaches a coherent ring-like structure (see Fig 2d).

The evolution to a ring, an eccentric ring at first, is important for the results of this study. The ring does not immediately spread into a disk because each of the particles is very small and gravitational interactions can only supply extremely small changes to eccentricities (collisional damping timescales are much shorter than viscous stirring timescales). Collisions between particles will damp energy, and conserve angular momentum, resulting in decreased eccentricities. Later, in Section 4, when accretion is included the ring-like structures start to spread when particles have grown to km-sized bodies and larger. Note that the eccentricity of the particles do not damp to zero because of the presence of the resonance. Also, due to the collisions, no particles are lost from the system despite the fact that many found themselves above the stability curve at times.

[EDITOR: Place Figure 2 here]

The evolution of each disk’s angular momentum is correlated with the collisional damping in each. Initially the averaged a_{eq} is at $\sim 2.87 a_{\text{Charon}}$, just inside the 5:1 MMR with Charon at $\sim 2.92 a_{\text{Charon}}$. This value rapidly increases, reaching $\sim 2.91 a_{\text{Charon}}$ on year-long timescales for the $R = 0.1$ km case plotted in Figure 2 (red triangles in Fig. 3). The amount of the increase depends strongly on the collisional evolution, which varies depending on the representative particle radii (ranging from 0.3 km to 0.01 km). We also ran a simple test case without collisions, which provides an upper bound to the outcomes shown here. The case with no collisions experienced the most dramatic outward movement of the ring’s angular momentum owing to absence of collisions to damp particles eccentricities (“No collisions” in Fig 3). There is a clear trend in outcomes as a function of the particle radii, as the systems with fewer collisions have the most extreme outward evolution of system angular momentum. The system with particles $R = 0.3$ km experienced on average 0.17 collisions per particle per orbit of Charon, which was roughly an order of magnitude less than the for the $R = 0.1$ km

system, with 1.7, and roughly 3 orders of magnitude less than the $R = 0.01$ km system which had 218 collisions per particle per Charon orbit.

[EDITOR: Place Fig 3]

A separate test removed the perturbations of Charon by examining the same disks of debris orbiting around a single central mass of mass equal to the combined mass of Pluto and Charon (see straight lines at $\sim 2.84 a_{\text{Charon}}$ in Fig 3). The results are plotted together with the those described above, and are distinct as they all show unchanging angular momentum as a function of time for each of the same three tested radii. This validates that, in the absence of external perturbation, the code conserves angular momentum as a population collisionally damps. It also shows that Charon is the cause of the angular momentum increase in our simulations.

We interpret that the dominating physical effect is that the timescale for inter-particle collisions is on order or shorter than the timescale for dynamical loss. In the collisionless system we find that more than half of the particles are ejected from the system due to Charon. As the collision rates increase from zero for this case to a few tenths (0.17 per particle per orbit for $R = 0.3$ km) and up to hundreds (for $R = 0.01$ km) not only are all particles kept in the system, but the outward evolution of the ring decreases. The longer that ring particles stay highly eccentric, the more close interactions they have with Charon, and the more chances to receive kicks to expand their orbits. Thus the lower collision rates are able to keep particles in the system, but they are still kicked substantially by Charon and the ring expands. By moving to higher collision rates (decreasing R) the ring damps faster, allowing less time for kicks from Charon and minimal expansion of the rings. We will find in more complex simulations in Section 4., that this outward movement of the ring works for eccentricities of Charon ranging from 0 to 0.3 and for a wide range of distances from Charon in terms if Charon’s orbital separation from Pluto.

What about the resonances? In Figure 4 we present results of similar disks of debris starting at a different semimajor axis relative to the barycenter of the Pluto-Charon system. Here the systems are evolving between the 4:1 or the 5:1 MMR. The results are slightly different. These disks start closer to Charon, and the increased perturbations

are evident with more extreme movement of the system’s angular momentum for a given particle size. However, the $R = 0.1$ km case moves more than the $R = 0.01$ km case, as would be expected given the two order of magnitude increase in collision frequency in the latter case. For the test cases further from Charon (starting between $2.8\text{--}2.9 a_{\text{eq}}$), the $R = 0.1$ km case and the $R = 0.01$ km case evolve to the same spot – near the 5:1 MMR. While the evolution of the $R = 0.3$ km case rapidly moved past the resonance, both of the more collisionally active cases show signs of resonant interactions with Charon. The smaller radii case had much more eccentricity damping and therefore a decreased semimajor axes. As the semimajor axes decreased the particles were converging with Charon allowing for resonant interactions (see Cheng 2011).

[EDITOR: Place Fig 4 here]

A similar series of test cases were created to provide a simplistic representation of a disrupted satellite (dubbed “simple disrupted satellite”). Here debris shares a similar point of origin on the orbit but has a range of a and e due to different initial ejection velocities away from the disrupted bodies orbit. Particles were distributed on orbits with a range of $a = 2.6\text{--}4.0 a_{\text{Charon}}$ and $e = 0.5\text{--}0.65$, but with similar pericenter values ($q \sim 1.35 a_{\text{Charon}}$) and similar longitude of pericenter value. In this test *all of the particles were initially on unstable orbits*, therefore without collisional interactions they would all be ejected from the system on very short timescales (< 10 years) despite Charon being on a zero eccentricity orbit. The particles had similar collisional properties described above ($R = 0.1$ km, with no growth or fragmentation).

The behavior of this disk is similar to the first test case, with the system rapidly (< 3 years) damping into a ring-like structure, this time near the 4:1 MMR. This system also experienced a large increase in angular momentum, circularizing near $\sim 2.5 a_{\text{Charon}}$, a substantial increase from the initial value of $\sim 2.25 a_{\text{Charon}}$.

[EDITOR: Place Fig 5 here]

As before, this same disk of debris was also modeled without collisions. The resulting evolution resulted in the ejection or accretion by Charon of over 60% of all the particles over the course of

the simulation and no coherent ring-like structure (see small, cyan, particles in upper panes of Fig 5).

These two simplistic test cases explored the powerful effects of collisional damping on the dynamical evolution of an eccentric ring. The tests showed that combined affects of dynamic perturbations from Charon and collisional damping of an eccentric ring can lead to outward movement of material in the system. This was one of the main problems in understanding the suite of small satellites in the Pluto-Charon system and this is a viable solution. While these tests only considered one value of disk semimajor axes and only one orbit for Charon (with different eccentricities in each test), the outcome of outward movement of material would scale to an epoch where Charon was closer to Pluto and still tidally evolving outward. In the case where a satellite was disrupted during the tidal evolution this outward movement would be very useful in helping to push the satellite outward without relying on any resonances to move material long distances in the system.

However, these simulations are missing the important physics of fragmentation and accretion that are necessary to understand where the disrupted satellite will re-build after it damps and moves out. High velocity collisions could create swarms of small debris that would dramatically change the collisional damping timescales of the large particles, while accretion during low relative velocity collisions could grow a few or many large bodies from the entire system. Where these bodies grow will show whether this mechanism can answer the second open question about the system, as to why the small satellites are located near resonances.

4. Disruption of a Primordial Satellite - Including Fragmentation and Growth

As shown in Section 3, collisional interaction between debris orbiting Pluto/Charon can radically change the collective dynamical behavior of an eccentric ring. Here we test similar scenarios with growth and accretion aiming to see if the collisionally evolving rings will preferentially grow near resonances, and we expand the study to investigate a wider range of initial ring locations relative to the orbit of Charon. There

are a few sources of such debris that could have played a role in the history of the Pluto-Charon system. Specifically, the simulations of Canup (2005,2011) find significant amounts of debris orbiting the Pluto-Charon system following their giant impact. Any debris that avoids accretion by Charon, survives dynamical ejection and accretes into satellites are then at risk of later dynamical ejection from the system during the outward tidal evolution of Charon (Lithwick and Wu 2008, Cheng 2011). The mechanism explored in the preceding Section can help to move material outward and avoid ejection but depends on the disruptions of satellites on similar timescales to the tidal evolution.

Mutual collisions between satellites are a possible means to disrupt bodies. Any satellites could have their eccentricities excited by entering or crossing MMRs, leading to crossing orbits and collisions (Cheng 2011, Cheng et al. 2014b). Collision velocities would be on order of a few 10’s m/s and approaching 100’s m/s as eccentricities get very high (Nix’s orbital velocity is ~ 140 m/s). However, lower velocity collisions may simply lead to accretion rather than disruption (a $R = 50$ km target needs to be hit by a $R \sim 43$ km projectile at 100 m/s to disrupt, using the \bar{Q}_D^* calculation from Benz and Asphaug 2009).

Heliocentric impactors are another method for disrupting any existing satellites and producing a significant amount of debris. In the environment where the collision probability for Charon’s formation was unity (*and nearly every large KBO appears to have suffered similar impacts*), then the lifetime of the smaller satellites ($R \sim 10 - 100$ km) could be much shorter than the time to dynamically deplete the Kuiper Belt (Levison et al. 2008) and possibly shorter than Charon’s tidal evolution timescale. The distribution of relative velocities for a heliocentric impactor depends on the dynamical state of the Kuiper Belt and could range from $\sim 100 - 500$ m/s (Pires dos Santos et al. 2012).

We start this series of calculations by generating the debris from the disruption of a satellite impacted by an object from an heliocentric orbit for use as initial conditions for our LIPAD simulations. We relied on an approximation by way of a N -body simulation of a 39 km radius object striking a 89 km radius body at 500 m/s with an impact angle of approximately 45 deg. The target body

was made of 9965 discrete, spherical and unbreakable particles and the impactor of 717 particles. The disruption event was modeled with the gravitational and granular mechanics code `pkdgrav`, which is commonly used for low-velocity impact modeling (see Leinhardt et al. 2000 and Richardson et al. 2000). This collision was done in a frame centered on the target-impactor center of mass. It was then translated into a frame relative to that of a satellite on different orbits around Pluto/Charon and with different orientations of the impact direction. This allowed for the exploration of collisions with a wide range of geometry relative to the velocity vector of the satellite. The specific collision modeled here is not derived from a collisional model, rather it was designed to be very general and have a high enough resolution and violent enough disruption to model the relevant physics in a wide range of cases.

The nature of the debris field causes a thin “tail” of debris that generally share a very similar pericenter (q) at the breakup location with a range of distributed, but correlated, a and e (similar configuration to the second of our simple disrupted satellite tests demonstrated above; Fig. 6a shows the collision outcome translated to the frame orbiting Pluto-Charon). The geometry tested most frequently in this work was when the impactor’s velocity vector was aligned with the target’s (satellite) velocity vector around Pluto-Charon. With this geometry some of the mass was immediately on orbits escaping the Pluto-Charon system, but most of the mass was on moderate eccentricity orbits ($e < 0.4$) within semimajor axis $\sim 4 a_{\text{Charon}}$. In the opposite geometry, when the impact velocity was anti-aligned with the satellite velocity, most mass was rapidly ejected from the system due to decreased pericenter distances and subsequent close encounters with Pluto or Charon.

In our main simulations we employed the complete fragmentation and growth capabilities of LIPAD. The simulations were started with 4096 tracer particles, each of mass 1.86×10^{14} kg, totaling 7.6×10^{17} kg in the system (Tholen et al. 2008 estimated a mass for Nix of 6×10^{17} kg). The smallest radius that a fragment could attain during a collision was 5×10^{-4} km, and the collisional routines used the Benz and Asphaug (1999) Q^* law for ice (line 4 in their Table III). The simulation used timesteps of 4×10^{-5} years, or about

21 minutes, which is ~ 437 timesteps per orbit of Charon.

This formula of taking the debris from a collision and placing them on a satellite’s orbit was repeated for different eccentricities of Charon, 0.0–0.3, and for different satellite semimajor axes $a = 2.2\text{--}2.8 a_{\text{Ch}}$. This grid of simulations was designed to test for the preferential growth of satellites in or near MMRs for a wide range of Charon orbital properties. Computational limitations did not allow for simulations to extend for the $\gg 1000$ years that might be necessary to allow each simulation to evolve to a single or stable system of satellites. Instead we consider the location of the angular momentum of the system of debris at the end of each run (typically at 200 years), as each run typically collisionally damped to a ring on the order of a few years allowed for the growth of large bodies in tens of years.

In all, 24 simulations were run to cover this parameter space, with significantly more test runs to examine the sensitivity of each to the various simulation parameters. The typical behavior is shown in Figure 6, where the particles initially have a radius of 0.01 km (some tests were run over an order of magnitude range of initial sizes and also using an initial size distribution with minimal differences in outcomes). The first few years were dominated by fragmentation where many particles grind down to the minimum allowable size. This is followed by a period of accretion due to their increased collisional damping leading to lower impact velocities (see the column forming in Fig 6b).

[EDITOR: Fig 6 here]

The location of the first collisions resulting in growth was important for the simulation outcomes (Fig 6c). The growth always started with the smallest particles as they have damped to very low eccentricity and experience low velocity collisions with each other. After the first accretion events there is rapid growth at the same location, building a “tower” structure in radius vs. semimajor axis space. The growth occurs in a very limited space, the “tower”, from this point forward where eventually the largest bodies in the system are built and most of the mass is in this structure. These structures are essentially ring structures where the fragmentation and collisional damping have limited much of the simulation mass to a narrow range of semimajor axis and subse-

quent growth at this spot is inevitable and then quite fast.

In Figure 6c the growth has reached ~ 10 km sized particles and most of the mass of the system resides in the larger (>1 km) particles with only a tail of smaller debris. The high eccentricity tail of debris is largely gone, and nearly all material is on low eccentricity ($e < 0.2$) orbits in a narrow range of semimajor axis. It has damped to a narrow ring. There are a few particles that appear to hug the 6:1 MMR at slightly higher eccentricity, suggesting that they are possibly being excited due to resonant interactions.

Finally in Figure 6d the ring has built enough large particles that it is now diffusing in semimajor axis. There are still a few particles seemingly excited by the 6:1 MMR, and also some particles that appear to have diffused inward and started interacting with the 5:1 MMR. The state of this simulation shows the complication in determining the endstate of these simulations. The angular momentum of this system is very near the 6:1 MMR, but the disk is clearly diffusing and not simply accreting into one or a few satellites. The build up at the 5:1 MMR may be an important process, but computational limits have frustrated further investigation.

The collisional environment that produces the evolution in Fig 6 produces fragmentation early when eccentricities are high, and accretion later after the disk has dynamically cooled into a ring. In a similar simulation the collisions suffered by one object were tracked, and the impact velocities as a function of time are plotted in Fig 7. During the first ~ 10 years of the disk’s evolution collisions are typically at or above 40 m/s, which is correlated with the large amounts of fragmentation found in Fig 6b, where the production of very small fragments is found. At later times the impact velocities become very low, less than ~ 10 m/s, as the system has dynamically damped into a ring with very low eccentricities. From this point, in Fig 6c accretion is found and correlates with these much lower velocities. Finally as the simulation approaches 1000 years the impact velocities slowly increase above 10 m/s, correlated with the ring spreading into a disk due to the presence of larger bodies ability to scatter smaller ones with some particles reaching higher eccentricities.

[EDITOR: Fig 7 here]

While some simulations result in rings of material near MMRs, it does not appear to be a systematic outcome when the final location of the ring’s angular momentum are plotted (see Fig. 8). A set of control cases were also run where the disruption debris was placed in orbit around a single central body that had the combined mass of Pluto and Charon. As expected, this case shows no preference for growth at any specific locations, and highlights some of the randomness in the location of the final ring of debris. The spacing and distribution of the final rings of debris is similar to that produced for both the cases of Charon eccentricity of 0.0 and 0.1, neither of which show any preference for growth at a MMR.

The case for Charon eccentricity of 0.3 was expanded and 3 additional initial conditions were tested, with initial orbits at $a = 1.9\text{--}2.1 a_{\text{Ch}}$. As expected, these closer cases were dynamically kicked outward and build rings at much more distant orbits (between the 5:1 and 6:1). The closer initial orbits led to increased loss of mass from the system as more of the initial ring distribution was on unstable orbits.

While there is no preference for growth near MMR, the movement outward of material is clearly seen here, as it was in the simple collision-only cases demonstrated previously. The tail of debris extends into regions of $a - e$ space that are unstable and thus there are substantial perturbations from Charon that drive the whole system outward. Meanwhile the collisions between disk particles are energetic enough to fragment particles which leads to substantial populations of small particles and enhances collisional damping of the system. This drives each system to damp on orbits further than the initial location of the disrupted satellite and a net movement outward of the system.

[EDITOR: Fig 8 here]

While this clearly shows the outward movement of material in the system for all Charon eccentricities examined, including $e_{\text{Ch}} = 0.0$, the suite of simulations were only run for one specific semi-major axis of Charon, that of today’s separation. Given that the stability region in $a - e$ space will scale with Charon’s orbit, the dynamical lifetimes should also scale with Charon’s orbit. The collisional timescales may change somewhat for closer orbits of Charon as the disrupted satellite at the

same distance in terms of Charon’s orbit a_{Ch} will fill less volume and have an increased collision rate. Our earlier tests explored 3 order of magnitude of collision rates and all found outward movement of material, so we expect that these results will apply throughout the tidal evolution of Charon.

5. Conclusions and Discussion

This work reports on a series of numerical experiments designed to understand the origin and evolution of the small satellites of Pluto. This work found that:

1. There are regions of stability in $a - e$ space, outside of which particles have very short survival timescales in the Pluto-Charon system if only gravitational interactions are considered. Collisions between particles can stabilize particles initially in the unstable region.
2. The combination of perturbations by Charon or particles reaching resonant orbits combine to increase angular momentum of a collisionally evolving disk of debris, moving the entire system outward.
3. Satellite disruption, and the subsequent collisional damping and re-accretion, does not lead to preferential formation in MMRs in the range of parameters tested in this work.

The satellite system of Pluto remains mysterious. As stated earlier, there are two major problems with the small satellites of Pluto, and we can report progress on one of the two. The first problem is that the satellites today are much more distant than can be explained by Charon-formation impact models. Here, by including collisional evolution in dynamical models, we have found that debris can experience substantial kicks from Charon while on unstable orbits, but then return to stable orbits due to collisions with other orbiting debris. This effect can result in the movement of material outward in the system.

The likelihood of this being an important process during the history of the Pluto-Charon system is not calculated, nor is it a trivial calculation as it requires a detailed understanding of the excitation, depletion and collisional evolution of

the Kuiper Belt. The tidal evolution timescale of Charon is on the order of a few million years and so collisional lifetimes must have been shorter than this for this to be important. However, it is expected that the Charon-forming collision happened in a different collision environment than found today in the Kuiper Belt and collisional timescales for ~ 100 km bodies must have been very short. Understanding the collisional history of both bodies by investigations with the *New Horizons* spacecraft mission may help to better understand these issues. This, in effect, suggests that today’s small satellites are essentially the last in multiple generations of previous satellites.

The second problem is the curious configuration of the small satellites, each near a MMR with Charon. There were indications in some simulations that collisionally active disks of debris would damp into a ring structure and could be caught while crossing a MMR (as found fortuitously in the simulation shown in Figure 6). However, a larger parameter space of simulations using a full fragmentation and accretion model failed to show a strong preference at any eccentricity of Charon. A large number of the simulation parameters were varied with none clearly indicating importance in a MMR capture mechanism. However, one curious outcome from these studies was the inner edge of a diffusing ring that interacts with a MMR. The importance of this effect could not be investigated here due to computational limitations, but could be potentially be responsible for building small satellites one MMR inward of a larger satellite.

Can success be claimed in the first problem and not the second? If collisional damping of an eccentric ring is necessary to move material outwards should it not also explain the orbital configuration? It is certainly possible that collisional evolution as tested here is not important or that there was another more dominant mechanism that could both move the satellites or their building blocks and result in their organized accretion near resonance. It is also possible that we have uncovered the means to move material outward in the system, and that there are more or different effects that will ultimately be responsible for the final orbital configuration.

Is it possible that we are simply being fooled by the system and that the orbital configuration is just luck? While four satellites near resonance is

hard to explain, both Kerberos and Styx both reside in relatively narrow regions of orbital stability (Pires dos Santos et al. 2012, Youdin et al. 2013). Nix and Hydra themselves are near a resonant configuration with each other, and so it is conceivable that Kerberos and Styx simply formed in the only places they could in a system with two more massive satellites that were somehow pushed into or near a resonance with each other.

Another question that this work can address with the tools developed here relates to the very first step of this entire process — the survival of any debris immediately following the formation of Charon. In the preceding Sections, we assumed that the post-impact debris measured by Canup (2011) would survive and remain in the Pluto-Charon system, despite the typically close orbits ($\sim 10 R_{\text{Pluto}}$) and the potentially high eccentricity of Charon. Using the same simulation configuration described above we have done a series of tests to estimate the collision rates necessary to stabilize debris at the formation distances found in Canup (2011). For a Charon eccentricity of 0.3, we considered disk masses of 6.75×10^{17} , 3.2×10^{17} and 1.2×10^{17} kg (Brozović et al. 2014 estimated $M_{\text{Nix}} + M_{\text{Hyd}} = 9.2 \times 10^{16}$ kg), placed on orbits at approximately $2 \times a_{\text{Charon}}$. This configuration is similar to the $a \sim 10 R_{\text{Pluto}}$ typically found for the debris relative to $a = 4 - 6 R_{\text{Pluto}}$ for Charon in Canup (2011). The simulations used the same collisional debris setup as explored in the previous Sections.

Only in the most massive case did significant amounts of debris survive. For 1.2×10^{17} kg only 5 particles were left at 500 years, and no coherent ring structure ever formed. Increasing to 3.2×10^{17} kg a very tenuous ring structure formed from the 70 particles that survived for 500 years, but for 6.75×10^{17} kg case over 800 particles remained, formed a ring, and experienced significant growth. The largest particle reached 4.8 km, and the recognizable “tower” structure grew between the 6:1 and 7:1 MMR.

These tests spanned the critical regime where the collision rate became high enough to keep debris in the system. The collision rates of 0.006, 0.039 and 0.102 collisions per particle per Charon orbit were found for the lowest to highest mass cases respectively, and thus a rate between the latter two values can be considered the critical limit

for survival of debris in this scenario. The Canup (2011) simulations found total masses of debris ranging from $10^{17} - 10^{21}$ kg (only 3 of 19 simulations were below 10^{18} kg). While the masses are typically above what was used in this test (with many simulations with 2–3 orders of magnitude higher mass), the collision rate will be the important quantity and will depend on the size distribution of debris in the system.

Looking beyond the Pluto-Charon system, some of the dynamical interactions between a massive perturber and a disk or ring of debris could be relevant on planetary scales. In our own Solar System the scattered disk of Kuiper Belt Objects shows the characteristic orbital features of having been excited by Neptune. In the context of this work, the dynamically excited scattered disk would have collisionally damped if the characteristic collisional timescales were shorter than the dynamical lifetimes.

Beyond our Solar System, there are circumbinary planets orbiting stellar systems with mass ratios similar to Pluto-Charon (see Kepler-16b reported in Doyle et al. 2011 and Kepler-34b and Kepler-35b reported in Welsh et al. 2012). Many of the effects driving planet formation in these systems will be different, particularly effects of the gaseous stellar nebula (see Meschiari 2014), but some of the orbital perturbations on the planetary building blocks will be of similar magnitude as those on satellite building blocks around Pluto and Charon.

In summary, this work has made progress on part of the confounding problems of the small satellites of Pluto. Hopefully this and other recent works, when combined with a very detailed study of the system by way of the *New Horizons* spacecraft mission (Stern 2008), will help to solve some of these outstanding mysteries.

K.J.W and H.F.L acknowledges support from NASAs NLSI (NNA09DB32A) and SSERVI (NNA14AB03A) programs that supported code development and H.F.L acknowledge support from NASA's OPR and OSS programs. This work used the Extreme Science and Engineering Discovery Environment (XSEDE), which is supported by National Science Foundation grant number ACI-1053575.

REFERENCES

- Beauvalet, L., Robert, V., Lainey, V., Arlot, J.-E., & Colas, F. 2013, *A&A*, 553, A14
- Benz, W., & Asphaug, E. 1999, *Icarus*, 142, 5.
- Braga-Ribas, F., and 63 colleagues 2014. *Nature*, 508, 72-75.
- Brown, M. E., & Schaller, E. L. 2007, *Science*, 316, 1585
- Brozović, M., Showalter, M. R., Jacobson, R. A., & Buie, M. W., 2014. *Icarus*, <http://dx.doi.org/10.1016/j.icarus.2014.03.015>
- Buie, M. W., Grundy, W. M., Young, E. F., Young, L. A., Stern, S. A. 2006. *AJ*, 132, 290-298.
- Buie, M. W., Tholen, D. J., Grundy, W. M. 2012. *LPSC*, 1667, 6249.
- Buie, M. W., Tholen, D. J., Grundy, W. M. 2012. *AJ*, 144, 15.
- Buie, M. W., Grundy, W. M., Tholen, D. J. 2013. *AJ*, 146, 152.
- Canup, R. M. 2005. A Giant Impact Origin of Pluto-Charon. *Science* 307, 546-550.
- Canup, R. M. 2011. *AJ*, 141, 35.
- Chambers, J. E., Wetherill, G. W., Boss, A. P. 1996. *Icarus*, 119, 261-268.
- Cheng, W. H., 2011, PhD thesis, Univ. of Hong Kong.
- Cheng, W. H., Lee, M. H., & Peale, S. J. 2014a, *Icarus*, 233, 242.
- Cheng, W. H., Peale, S. J., & Lee, M. H. 2014b, *Icarus*, 241, 180.
- Desch, S. J. 2014. Lunar and Planetary Science Conference 45, 1135.
- Dobrovolskis, A. R. 1989, *Geophys. Res. Lett.*, 16, 1217.
- Doyle, L. R., and 48 colleagues 2011. *Science*, 333, 1602.

- Duncan, M. J., Levison, H. F., & Lee, M. H. 1998, *AJ*, 116, 2067.
- Dvorak, R., Froeschle, C., & Froeschle, C. 1989, *A&A*, 226, 335.
- Farinella, P., Milani, A., Nobili, A. M., & Valsecchi, G. B. 1979, *M&P*, 20, 415.
- Holman, M. J., Wiegert, P. A. 1999. *AJ*, 117, 621-628.
- Kenyon, S. J., & Bromley, B. C. 2014, *AJ*, 147, 8
- Lee, M. H., Peale, S. J. 2006. *Icarus*, 184, 573-583.
- Leinhardt, Z. M., Richardson, D. C., & Quinn, T. 2000, *Icarus*, 146, 133.
- Lellouch, E., Sicardy, B., de Bergh, C., et al. 2009, *A&A*, 495, L17.
- Levison, H. F., Morbidelli, A., Van Laerhoven, C., Gomes, R., & Tsiganis, K. 2008, *Icarus*, 196, 258.
- Levison, H. F., Duncan, M. J., & Thommes, E. 2012, *AJ*, 144, 119.
- Lithwick, Y., & Wu, Y. 2008, arXiv:0802.2951
- McKinnon, W. B. 1989. *ApJ*, 344, L41-L44.
- Meschiari, S. 2014. *The Astrophysical Journal*, 790, 41.
- Peale, S. J. 1999, *ARA&A*, 37, 533.
- Peale, S. J., Cheng, W. H., Lee, M. H. 2011. EPSC-DPS Joint Meeting, 2011, 665.
- Pires Dos Santos, P. M., Giuliatti Winter, S. M., Sfair, R. 2011. *MNRAS*, 410, 273-279.
- Pires dos Santos, P. M., Morbidelli, A., Nesvorný, D. 2012. *CeMDA*, 114, 341-352.
- Richardson, D. C., Quinn, T., Stadel, J., & Lake, G. 2000, *Icarus*, 143, 45
- Showalter, M. R., Hamilton, D. P., Stern, S. A., Weaver, H. A., Steffl, A. J., Young, L. A. 2011. *CBET*, 2769, 1.
- Showalter, M. R., and 10 colleagues 2012. AAS/Division for Planetary Sciences Meeting Abstracts, 44, #304.07.
- Sicardy, B., Bellucci, A., Gendron, E., et al. 2006, *Nature*, 439, 52
- Stern, S. A., Parker, J. W., Duncan, M. J., Snowdall, J. C., Jr., & Levison, H. F. 1994, *Icarus*, 108, 234
- Stern, S. A., Bottke, W. F., Levison, H. F. 2003. *AJ*, 125, 902-905.
- Stern, S. A., Weaver, H. A., Steffl, A. J., Mutchler, M. J., Merline, W. J., Buie, M. W., Young, E. F., Young, L. A., Spencer, J. R. 2006. *Nature*, 439, 946-948.
- Stern, S. A., Mutchler, M. J., Weaver, H. A., Steffl, A. J. 2007. *LPSC*, 38, 1722.
- Stern, S. A. 2008. *SSRv*, 140, 3-21.
- Tholen, D. J., Buie, M. W., Grundy, W. M., Elliott, G. T. 2008. *AJ*, 135, 777-784.
- Ward, W. R., Canup, R. M. 2006. *Science*, 313, 1107-1109.
- Weaver, H. A., Stern, S. A., Mutchler, M. J., Steffl, A. J., Buie, M. W., Merline, W. J., Spencer, J. R., Young, E. F., Young, L. A. 2006. *Nature*, 439, 943-945.
- Welsh, W. F., and 45 colleagues 2012. *Nature*, 481, 475-479.
- Wisdom, J., & Holman, M. 1991, *AJ*, 102, 1528.
- Youdin, A. N., Kratter, K. M., Kenyon, S. J. 2012. *ApJ*, 755, 17.

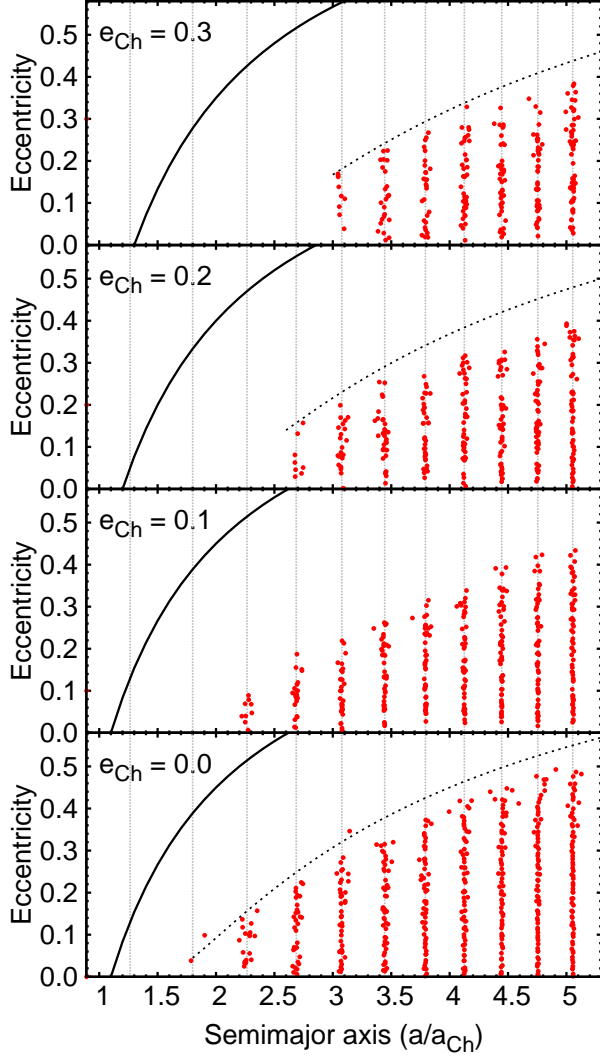


Fig. 1.— Survival of particles orbiting Pluto and Charon as a function of their initial a and e , and the eccentricity of Charon, e_{Ch} . The smallest dots (black) represent the initial distribution of orbits for test particles at time=0 and the largest dots (red) show their orbits after 1000 years. Empirical curves are drawn as an envelope to the stable regions for a circular orbit of Charon (bottom frame), and for a Charon eccentricity of $e_{\text{Charon}} = 0.3$ (top frame).

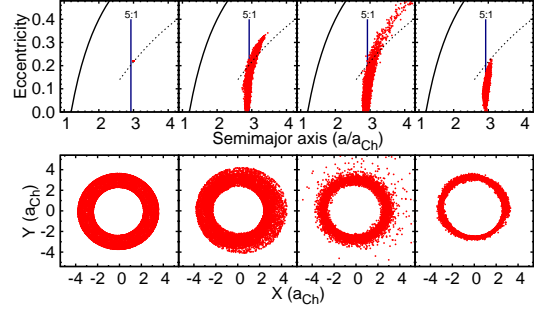


Fig. 2.— Frames showing the collisional damping of a “simple eccentric disk” of debris at times (from left to right) 0, 0.1, 0.5, and 3.0 yr. The angular momentum of the system increases due to kicks from Charon and also the resonant interactions of the ring with Charon’s orbit while the disk damps into a ring. Note that the structure seen in the ring in the last frame shows that it is interacting with the resonance.

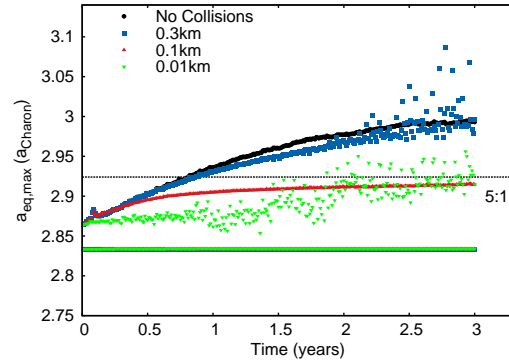


Fig. 3.— The temporal evolution of the angular momentum of our eccentric rings as represented by a_{eq} . The colors indicate particle sizes, as shown in the legend. However, the black symbols show a control run where collisions were ignored. The figure shows two calculation for each particle size. The upper curves are systems with Charon. The lower curves (which are horizontal lines indicating that angular momentum is conserved) has a single central body. Note that all four of the latter runs overlap in the figure. The dotted line shows the location of the 5:1 MMR with Charon.

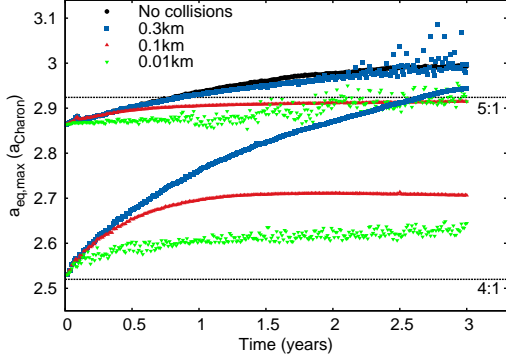


Fig. 4.— The top set of lines are the same as in Figure 3. The bottom set of data is the identical experiment with similar disk and particle properties, but with the disk starting closer to Pluto-Charon and evolving in between resonances, rather than starting near the 5:1 MMR.

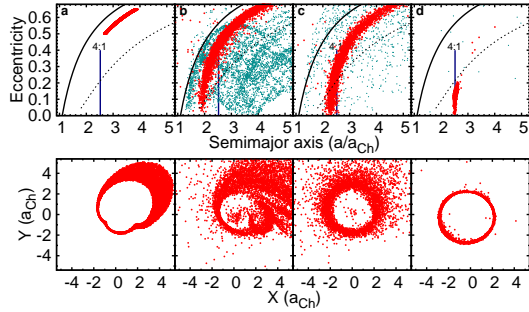


Fig. 5.— Frames showing the collisional damping of a disk of debris with initially correlated periapsis q , and a range of a and e at times (from left to right) 0, 0.1, 0.5, and 3.0 yr. All of the particles are initially on unstable orbits and with semimajor axes exterior to the 4:1 MMR. The angular momentum of the system increases due to kicks from Charon and also the resonant interactions of the ring with Charon’s orbit. Most particles cross the 4:1 MMR while damping semimajor axis, and the final ring structure is resonating with Charon in the 4:1 MMR. The cyan particles (smaller point sizes in the top frames only) are from a simulation with the same initial conditions, but with no collisions. They are rapidly dispersed and lost from the system.

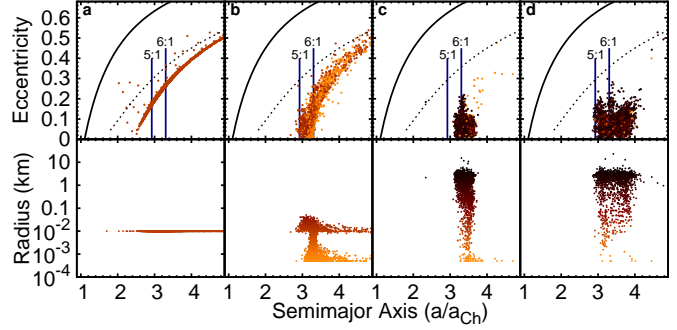


Fig. 6.— Evolution of a disrupted satellite, where Charon has an eccentricity of 0.2, and the satellite was disrupted at 48,000 km from the Pluto-Charon barycenter on a zero eccentricity orbit. The dotted line in the top panels signifies the stability boundary, the solid line marks where an orbit’s pericenter crosses Charon and the major MMRs are labeled. The bottom panels shows the size of the particles, where here they were initially 0.01 km, and were allowed to break to a minimum size of 10^{-4} km. The colors represent their radius, with particles above 1 km being black. The plots represent the evolution of the system at 0.0, 5, 100, and 400 years.

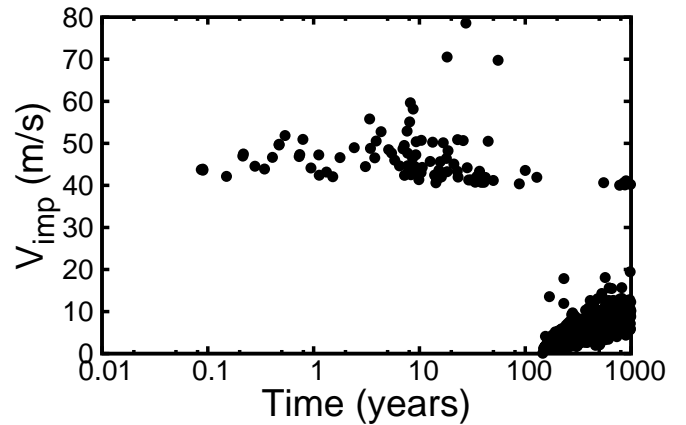


Fig. 7.— Impact velocities as a function of time for a single particle in a simulation similar to that shown in Fig 6.

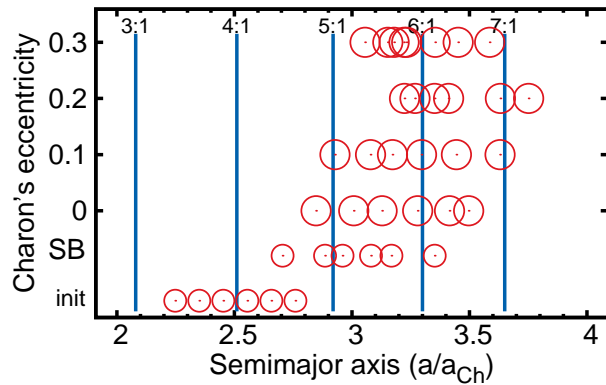


Fig. 8.— Summary of the location of the circularized angular momentum of the remaining debris after 200 years for a range of Charon eccentricity and initial satellite location. The y-axis nominally indicates the eccentricity of Charon for each represented simulation, with “SB” indicating simulations where the mass of Charon was added to Pluto and the simulation was run around a single massive body. The locations marked by “init” are the locations of the initial disrupted satellite.